Research Article

Ectopic expression of a rice triketone dioxygenase gene confers mesotrione tolerance in soybean

Shunhong Dai,[*] **Nikolaos Georgelis, Mohamed Bedair, Yun-Jeong Hong, Qungang Qi, Clayton T Larue, Bikram Sitoula, Wei Huang,**[†] **Brian Krebel, Michael Shepard, Wen Su, Keith Kretzmer, Jiaxin Dong, Thomas Slewinski, Sarah Berger, Christine Ellis, Agoston Jerga and Marguerite Varagona**

Abstract

BACKGROUND: Herbicide-resistant weeds pose a challenge to agriculture and food production. New herbicide tolerance traits in crops will provide farmers with more options to effectively manage weeds. Mesotrione, a selective pre- and post-emergent triketone herbicide used in corn production, controls broadleaf and some annual grass weeds via hydroxyphenylpyruvate dioxygenase (HPPD) inhibition. Recently, the rice HIS1 gene, responsible for native tolerance to the selective triketone herbicide benzobicyclon, was identified. Expression of HIS1 also confers a modest level of mesotrione resistance in rice. Here we report the use of the HIS1 gene to develop a mesotrione tolerance trait in soybean.

RESULTS: Conventional soybean is highly sensitive to mesotrione. Ectopic expression of a codon-optimized version of the rice HIS1 gene (TDO) in soybean confers a commercial level of mesotrione tolerance. In TDO transgenic soybean plants, mesotrione is rapidly and locally oxidized into noninhibitory metabolites in leaf tissues directly exposed to the herbicide. These metabolites are further converted into compounds similar to known classes of plant secondary metabolites. This rapid metabolism prevents movement of mesotrione from treated leaves into vulnerable emerging leaves. Minimizing the accumulation of the herbicide in vulnerable emerging leaves protects the function of HPPD and carotenoid biosynthesis more generally while providing tolerance to mesotrione.

CONCLUSIONS: Mesotrione has a favorable environmental and toxicological profile. The TDO-mediated soybean mesotrione tolerance trait described here provides farmers with a new option to effectively manage difficult-to-control weeds using familiar herbicide chemistry. This trait can also be adapted to other mesotrione-sensitive crops (e.g. cotton) for effective weed management.
© 2022 Bayer Crop Science. Pest Management Science published by John Wiley & Sons Ltd on behalf of Society of Chemical Industry.

Supporting information may be found in the online version of this article.

Keywords: triketone dioxygenase (TDO); mesotrione; herbicide tolerance trait; hydroxyphenylpyruvate dioxygenase (HPPD); phytene desaturase (PDS); carotenoids

1 INTRODUCTION

Increasing sustainable crop production is crucial to meet the needs of food for the growing global human population, feed for increased demand for animal-based diets in developing nations, and the expanded use of crop products to produce biofuel, fiber, and other agricultural product-based commodities, while using limited natural resources.[1] Weed control is one of the major challenges to sustainable crop production. Herbicide application is an important method to reduce weed pressure, improve productivity, and increase security for global crop production. Selective herbicides were major contributors to improve crop production before the deployment of herbicide-tolerant

(HT) crops.[2,3] The cultivation of HT crops coupled with the application of corresponding herbicides can effectively manage weeds, improve crop productivity and quality, enhance the content of soil organic matter, improve soil health, and reduce fuel consumption and emission by reducing tillage.[2–5]

* Correspondence to: S Dai, Bayer Crop Science, 700 Chesterfield PKWY W, Chesterfield, MO 63017, United States. E-mail: shunhong.dai@bayer.com

† Present address: Current address: Corteva Agriscience, 9330 Zionsville Road, 306/A2-727, Indianapolis, IN, 46268, United States

Deployment of glyphosate tolerant (GT) crops, alongside application of glyphosate, revolutionized modern agriculture by providing an effective alternative to using traditional selective herbicides for weed control.[6] GT crops were the most rapidly adopted technology in the history of agriculture, which was primarily due to the nonselective, very effective, and relatively inexpensive nature of glyphosate.[2,7,8] Better weed control in GT crops improved crop production efficiency, e.g. growing GT soybean resulted in an average yield increase of 7% in developed countries and 21% in developing countries with smallholder farmers.[2,8]

Due to the intensive use of herbicides for general weed control, the number of weed species resistant to one or more herbicide sites of action (SOA) has steadily increased (http://www.weedscience.org/)[9]. Broad adoption of GT crops coupled with the concurrent application of glyphosate has also caused an increased number of glyphosate-resistant weed species.[10] Herbicide resistance increases the cost of weed management and limits herbicide options to control some resistant weeds.[9,11] Developing and deploying crops with tolerance to diverse herbicide SOAs as trait stacks is essential to enable farmers to effectively manage weeds. Crops with stacked herbicide tolerance traits will also help slow the pace of herbicide resistant weed evolution.[3,12,13]

Hydroxyphenylpyruvate dioxygenase (HPPD) inhibitors are among the newest herbicide SOAs following their introduction in the 1980s.[13,14] HPPD irreversibly converts hydroxyphenylpyruvic acid (HPPA) into homogentisic acid (HGA) in plants. HGA is the substrate to produce α-tocopherols (vitamin E, important for protecting biological membranes against oxidative stress and the photosynthetic apparatus against photo-inactivation), plastoquinone [PQ, a cofactor of phytoene desaturase (PDS), important for carotenoid biosynthesis and protection of photosynthesis], and acetoacetate for central metabolism.[15–17] HPPD-inhibiting herbicides abrogate tyrosine degradation in nonresistant plants, which subsequently stops the production of PQ and vitamin E, negatively affects carotenoid biosynthesis, causes leaf bleaching symptoms, and ultimately leads to plant death.[14,18]

Mesotrione, a β-triketone herbicide, is an extremely potent competitive inhibitor of HPPD. In weed species it is rapidly absorbed following foliar application, translocated acropetally and basipetally, and causes severe bleaching symptoms and plant death.[18] Originally developed as a selective herbicide for controlling weeds in corn, mesotrione provides pre- and post-emergence control of important broad-leaf and some annual grass weeds.[18] Mesotrione has pre-emergence activity ranging from 4.5 to 32 days, depending on soil pH, and shows no risk of carry-over in rotational crops.[18–20] Because of the favorable environmental and toxicological profiles, mesotrione and other HPPD inhibitors were considered 'reduced risk pesticides' by the US Environmental Protection Agency.[21]

While useful in corn, mesotrione cannot be used to manage weeds in many other crops (e.g. soybean) due to the sensitivity to this herbicide.[18] Maeda et al. identified the rice HPPD INHIBITOR SENSITIVE 1 (HIS1) gene, which is responsible for the tolerance to benzobicyclon, based on varietal variation in sensitivity to this selective herbicide.[22] HIS1, encoding a 351 amino acid Fe(II)/2-oxoglutarate-dependent oxygenase, can also confer a modest level of tolerance to other β-triketone herbicides in rice, including mesotrione.[22] In this study we report our efforts on utilizing the rice HIS1 gene to develop a mesotrione tolerance trait in soybean. The rice HIS1 was codon optimized for better expression in soybean, and the optimized version of HIS1 is designated as

TDO (Triketone dioxygenase gene). TDO transgenic soybean plants showed strong tolerance to mesotrione (up to 16× the commercial application rate). Ectopic expression of TDO in soybean showed no other effects on plant growth and development. Ectopically expressed TDO rapidly converts mesotrione into non-inhibitory compounds at the point of application that are further catabolized into metabolites that are similar to known classes of plant secondary metabolites. Rapid and local turnover of mesotrione in TDO transgenic soybean plants prevents mesotrione moving from treated leaves to vulnerable emerging leaf tissues and inhibiting the function of HPPD. This rapid metabolism of mesotrione protects the function of PDS and carotenoid biosynthesis and prevents mesotrione-induced herbicide injury. Ectopic expression of TDO in soybean resulted in commercial-level mesotrione tolerance for an HT trait that will provide growers with more options in managing difficult-to-control weeds.

2 MATERIAL AND METHODS

2.1 Cloning of TDO transformation constructs and developing TDO transgenic soybean plants

The coding sequence of TDO (GenBank accession number: ON092642) was amplified via PCR with the primers Dna-HIS1-F (5′-CTTGTTTGTTGATTGAGAATAGGATCC-ATGGCTGACGAGTCAT GGAGGGC-3′) and Nos-HIS1-R (5′-GCCAAATGTTTGAACGAT CAATTC-TCAGATCCTCAGGGAGTCGATGTACC-3′) using a pET28-based TDO protein expression vector as the template.[23] The amplified PCR fragment was cloned into a plant expression binary vector via the BamHI site using hot-fusion cloning, which resulted in p35S::TDO. p35S::TDO carries two cassettes: one with TDO driven by an enhanced 35S promoter (e35S:TDO:Nos) and another one for streptomycin selection. Transgenic soybean events carrying T-DNA of p35S::TDO were developed through Agrobacterium-mediated transformation as previously described.[12] The TDO copy number was determined via a Taqman assay. Events carrying a single copy TDO insertion were used for herbicide tolerance and biochemical assays in this study.

2.2 Mesotrione tolerance assay

Plants from homozygous lines of p35S::TDO transgenic events 116, 125, and 129, and the conventional soybean control, were grown in 3.5″ pots using soybean potting media in a growth chamber under the following conditions: 28 °C/24 °C (light/dark) and 16 h light at 700 μE/8 h dark photoperiod and fertilized with Peters general purpose fertilizer. Uniform V4 growth stage plants were sprayed with mesotrione (diluted from Callisto with 1% crop oil) at 1×, 2×, 4×, 8×, and 16× the commercial rate (1× = 105 g ha^{-1} of active ingredient) to evaluate mesotrione tolerance. Eight plants per entry were used in each treatment. Crop injury was rated 13 days after mesotrione treatments.

2.3 Biochemical quantification of ^{14}C-mesotrione absorption and movement

Plants from transgenic event 125 of p35S::TDO and the control were grown under the conditions described above. V1 growth stage plants were first sprayed with 1X nonradiolabeled mesotrione and followed by application of 12 × 2 μL droplets of ^{14}C-mesotrione solution, formulated from [phenyl-U-^{14}C] mesotrione (4.627 MBq mg^{-1}) (Institute of Isotopes Co., Ltd, Izotop, Budapest, Hungary) in 1% crop oil, to the adaxial surface of the first trifoliate of each plant (1.8 μg per plant). Plants were sampled at 1, 3, 6, 24,

and 72 h after treatment (HAT), four plants/entry/time point. Four samples were collected from each plant: treated first trifoliate, apex (all tissues above the first trifoliate), unifoliate (all above ground tissues under the node of the first trifoliate), and roots. The treated first trifoliate was washed with 80% acetonitrile to remove unabsorbed herbicide and air dried. Root samples were separated from soil, washed, and dried with paper towels. All samples were weighed, frozen in liquid nitrogen, and stored at −80 °C until analysis.

Samples were milled on dry ice and extracted by adding 80% acetonitrile in a 1:10 ratio of sample weight to extraction solution, homogenized using a Geno/Grinder 2010 (SPEX SamplePrep) for 20 min and centrifuged. After transferring supernatants to new tubes, each pellet was resuspended in 50% acetonitrile for a second extraction as described above. Supernatants from both extractions were combined, and radioactivity in each sample was quantified using a Liquid Scintillation Analyzer (Perkin Elmer Tri-Carb 2900TR) with Ultima Gold scintillation liquid (PerkinElmer). The percentage radioactivity of each sample type was calculated by dividing the radioactivity recovered in the sample type by the total radioactivity recovered in all samples of the plant.

2.4 Radiography of the translocation of ^{14}C-mesotrione and its derivatives

V1 growth stage plants of event 125 of p35S::TDO and the control (six plants/entry) were sprayed with 1× nonradiolabeled mesotrione followed by applying 40 μg of ^{14}C-mesotrione droplets to the first trifoliate using a 0.5 μg μL^{-1} ^{14}C-mesotrione solution in 1% of crop oil. Plants were pulled out of pots at 30 HAT and, after soil was washed from the roots, placed in cassettes, imaged and exposed to phosphoscreens. After 2–3 weeks of exposure in −80 °C, the phosphoscreens were scanned at 50 μm resolution using a Personal Molecular Imager (PMI)-FX (Bio-Rad).

2.5 Biochemical analysis of mesotrione movement and its inhibition of HDDP using nonradiolabeled mesotrione

V1 growth stage plants of p35S::TDO events 125 and 129, and the control were used for mesotrione treatments. Plants with their apex (all tissues above the node of the first trifoliate) covered by aluminum foil were sprayed with 2× mesotrione. After the leaves were air dried, the aluminum foil was removed and the first trifoliate and apex (covered by aluminum foil at spray) of each plant were sampled separately at 1, 3, 6, 24, and 72 HAT, respectively. Tissues from two plants were pooled as one sample and three replicates/entry/time point were collected, frozen in liquid nitrogen, and stored at −80 °C until analysis.

The frozen samples collected above were milled frozen and lyophilized. On average, about 20 mg of each lyophilized sample was extracted in 1 mL of 80% methanol for 7 h at 4 °C and centrifuged. Then 200 μL of supernatant from each sample was diluted to 450 μL with 20% methanol for analysis. Mesotrione, hydroxy-mesotrione, 4-(methylsulfonyl)-2-nitrobenzoic acid (MNBA), 2-amino-4-(methylsulfonyl) benzoic acid (AMBA), HPPA, and HGA were analyzed using an ultra-performance liquid chromatography–tandem mass spectrometer (UPLC–MS/MS) system consisting of a Shimadzu UPLC system and an AB Sciex 5500 triple quad mass spectrometer. Separation was achieved using an AQUITY UPLC BEH C18 column, 1.7 μm, 2.1 × 100 mm (Waters) maintained at 40 °C, with an injection volume of 5 μL. The mobile phase consisted of solvent A (0.1% vol/vol aqueous formic acid) and solvent B (0.1% vol/vol formic acid in acetonitrile). The mobile

phase gradient was initially set at 5% B and increased linearly to 60% B in 8 min at a flow rate of 0.3 mL min^{-1}. Mesotrione and hydroxy-mesotrione were analyzed in positive MRM mode, precursor to products ions were 340.0 to 228.0 Da for mesotrione, and 356.0 to 228.0 Da for hydroxy-mesotrione. MNBA, AMBA, HPPA, and HGA were analyzed in negative MRM mode, precursors to product ions were 244.0 to 200.0 Da for MNBA, 214.0 to 170.0 Da for AMBA, 179.0 to 107.0 Da for HPPA, and 167.0 to 123.1 Da for HGA. Data was processed, including peak picking and integration, using Analyst Software (Sciex). All compounds measured were quantified using an external calibration curve of their respective standard except hydroxy-mesotrione, which was quantified using the external calibration curve of the mesotrione standard.

2.6 Identification and quantitation of mesotrione-derived metabolites

Two experiments were conducted to identify and quantify mesotrione-derived metabolites. To identify mesotrione derivatives, the first trifoliates of event 125 of p35S::TDO and the control plants at the V1 growth stage were treated with 60 μg/plant of radiolabeled mesotrione solution droplets containing ^{13}C-mesotrione (WuXi AppTec Co., Ltd) and ^{14}C-mesotrione (Izotop) at a ratio of 0.55 in 28% acetonitrile and 1% crop oil, three replicates/entry/time point. Treated trifoliates were sampled at 3, 24, and 74 HAT, washed with 80% acetonitrile, air dried, weighed, and stored at −80 °C until analysis. Samples were ground using a Geno/Grinder 2010 at 1500 rpm for 10 min after adding 10 mL of 80% acetonitrile extraction solution and three 4-mm stainless ball bearings to each sample and centrifuged at 3500 rpm (Eppendorf centrifuge 5810R) for 10 min after grinding. Supernatants were transferred to new tubes and pellets were extracted two more times (three extractions in total) by repeating the above steps using 10 mL of 80% acetonitrile solution and 10 mL of 50% acetonitrile extraction solution, respectively. Supernatants from all three extractions of the same sample were combined and all samples were evaporated to dryness using a Genevac EZ-2.3 Elite (HCl compatible, SP scientific) with option 08: High + Low BP at 40 °C maximum temperature. Each dried sample was resuspended in 1.5 mL of LC/MS grade water. Finally, 100 μL of each sample was filtered through a 0.45 μm modified nylon centrifugal filter (VWR) and loaded into an amber glass HPLC vial for analysis.

To quantify mesotrione-derived metabolites, V1 growth stage plants were sprayed with 1X nonradiolabeled mesotrione, immediately followed by application of 40 μg of ^{14}C-mesotrione droplets on the adaxial surface of the first trifoliate of each plant using a 0.5 μg/μL ^{14}C-mesotrione solution in 1% of crop oil. ^{14}C-mesotrione-treated first trifoliates were sampled at 1, 6, 24, and 72 HAT, washed with 80% acetonitrile, and stored at −80 °C, four replicates/entry/time point. Samples were extracted using the same method as for the ^{13}C-/^{14}C-mesotrione experiment for biochemical analysis presented above.

An Agilent 1290 Infinity HPLC system with temperature-controlled autosampler (15 °C) and a Waters XBridge Shield RP18 column (3.5 μm, 4.6 × 250 mm) at 30 °C were used to separate the extracts (see Supporting Information for details about the mobile phase and injection volumes). A valve (Analytical Scientific Instruments Model: 600-PO10-04) was used to split the outcoming flow to a radioactivity (RAD) detector (β-RAMmodel5) and a Q-Exactive HF High Resolution mass spectrometer system at a ratio of 2:1. The flow that went into the RAD detector was mixed with 2.1 mL min^{-1} of Flowlogic U liquid (LabLogic Systems Inc.).

For mass spectrometer detection, details of MS parameters are listed in the Supporting Information. In addition to the FullScan/ddMS2-positive mode, a set of selected samples was run in the negative mode for mass detection (see Supporting Information for MS parameters). To obtain more complete MS2 data for selected candidate precursor ions, a Full Scan-PRM mode was run on selected ^{14}C-mesotrione-treated samples using the same tuning parameters as for positive mode (details of MS parameters are presented in the Supporting Information). The post-column flow after sample injection was collected for the full 60 min gradient, and the radioactivity was measured and compared with the radioactivity before injection using a Liquid Scintillation Analyzer (PerkinElmer Tri-Carb 2900TR) with Ultima Gold scintillation liquid (PerkinElmer). The recovery rate of ^{14}C radioactivity after injection was >90% (data not shown).

In the [13]C- and ^{14}C-mesotrione study to identify metabolites, raw data was processed using the Expected and Unknown Met ID Workflow with MMDF for complex matrixes samples within Compound Discoverer 3.1 (Thermo Fisher Scientific). Candidate mesotrione derivatives were identified by taking advantage of their enriched ^{13}C/^{12}C ratio and alignment of HPLC/RAD and HPLC/MS–MS signals. In the ^{14}C-mesotrione study for metabolite quantification, mesotrione derivatives were quantified by expressing the radioactivity count area of the individual metabolite as a percentage of the total radioactivity count of the whole sample in the HPLC/RAD/MS–MS analysis. Quantitation of count areas and generation of radioactivity graphs was done using Laura software 4.2.6.79 (LabLogic). MS peak areas were measured using Quant-Browser within XCalibur software 4.3 (Thermo Fisher Scientific). The list of mesotrione derivatives was narrowed down to the compounds that contributed 1–2% or more to the total radioactivity counts of ^{14}C-mesotrione-treated samples. Strong positive correlation between radioactivity count and MS signal areas of individual mesotrione-related compounds provided additional support for the identity of the compounds. Putative identities of mesotrione derivatives were proposed based on accurate MS1 and MS2 similarities among compounds in this study as well as comparisons with published MS2 spectra on mesotrione derivatives. Commercial standards for AMBA (AMBEED) and MNBA (ACCELA), and 5-hydroxy-mesotrione, produced by TDO protein mediated *in-vitro* reaction and verified by NMR analysis,[23] were used to confirm the identification of the specific metabolites.

2.7 Quantitation of phytoene, carotenoids, and chlorophylls

V1 growth stage plants were sprayed with 2× mesotrione. The apex and first trifoliate of each plant were sampled at 30 HAT, three replicates/entry, frozen in liquid nitrogen and stored at −80 °C until analysis. After milling and lyophilization, ~20 mg of each milled sample was transferred into a 2-mL vial and weighed. Next 1 mL of extraction solvent (acetone:ethyl acetate, 3:2 v/v) was added to each vial, and the vials were then capped and shaken at room temperature for 1 h. After shaking, 0.8 mL of water was added to each vial and they were capped, mixed vigorously, and centrifuged at 1000 rpm for 10 min. Finally, 200 μL of the supernatant in each vial was transferred to an HPLC vial with a fused insert, capped immediately, and stored with light protection prior to analysis. An Agilent HPLC system with the column temperature set at 35 °C and the autosampler temperature at 10 °C was used to analyze carotenoids, chlorophylls, and phytoene using a YMC Carotenoid C30 column (5.0 μm, 4.6 × 250 mm) with different mobile phases and gradient profiles.

For the analysis of phytoene, the sample injection volume was 20 μL (see Supporting Information for details of mobile phase, flow rate, and gradients). Phytoene was detected at 286 nm and eluted at 5.0 min. An (E/Z)-phytoene standard (Sigma-Aldrich) was dissolved/diluted with ethyl acetate to establish a calibration range of 0.04–5.0 ng μL.

For the analysis of carotenoids and chlorophylls, the sample injection volume was 10 μL (see Supporting Information for details of mobile phase, flow rate, and gradients). Solutions of standards (from Chromadex and Sigma-Aldrich) were prepared using ethyl acetate. The detection wavelengths, retention times, and calibration ranges for each compound are listed in the Supporting Information.

3 RESULTS

3.1 Ectopic expression of TDO in soybean confers a commercial level of mesotrione tolerance

It was previously shown that the rice *HIS1* gene confers tolerance to multiple triketone herbicides in rice, including mesotrione,[22] although the level of tolerance was not evaluated to determine whether *HIS1* is a viable option for HT trait development. To test whether ectopic expression of *HIS1* in soybean can confer sufficient tolerance to mesotrione for an HT trait, transgenic soybean plants were developed from a set of binary vectors carrying codon optimized *HIS1* (*TDO*) driven by different promoters. Among events tested, transgenic events carrying p35S::TDO with *TDO* driven by an enhanced 35S promoter conferred a commercial level of mesotrione tolerance. As shown in Fig. 1(A),(C), events with similar levels of TDO (Fig. S1) can tolerate up to 16× the commercial application rate of mesotrione while conventional soybean plants were severely injured by mesotrione at any rates applied, from 1× to 16× ((A) *versus* (B) in Fig. 1). The herbicide injury ratings of all *TDO* transgenic events were lower than 10% when plants were treated with 1× to 8× mesotrione (Fig. 1(C)). The herbicide injury ratings of p35S::TDO events remained below 15% after plants were treated with an ultra-high dose of mesotrione (16×) (Fig. 1(C)). Because these *TDO* transgenic events had similar levels of TDO expression and effects on mesotrione tolerance (Figs S1 and 1(C)), events 125 and 129 were used in non-radiolabeled biochemical studies, and only event 125 was used in the radiolabeled biochemical experiments described in the following.

3.2 Systemic movement of mesotrione is limited in soybean plants overexpressing TDO

Mesotrione moves acropetally and basipetally in susceptible weeds.[18] To evaluate the effect of overexpression of *TDO* on mesotrione movement, droplets of ^{14}C-mesotrione solution were applied to the adaxial epidermis of the first trifoliate at the V1 growth stage. Systemic movement was observed in conventional soybean plants, but not *TDO* transgenic plants in radiographs of ^{14}C-mesotrione-treated plants (Fig. 2(A)). In conventional soybean plants, translocation and accumulation of radioactivity were detected in leaf tissues above the treated trifoliate, especially in new emerging leaves, at 30 HAT, while trace amounts of radioactivity moved to the hypocotyl and roots (Fig. 2(A)). In contrast, no translocation of radioactivity to other body parts was detected in *TDO* transgenic plants, and all detectable radioactivity was retained in the treated first trifoliate (Fig. 2(A)).

To quantify the relative amount of mesotrione and its derivatives that moved out of the treated leaf, a time course study was
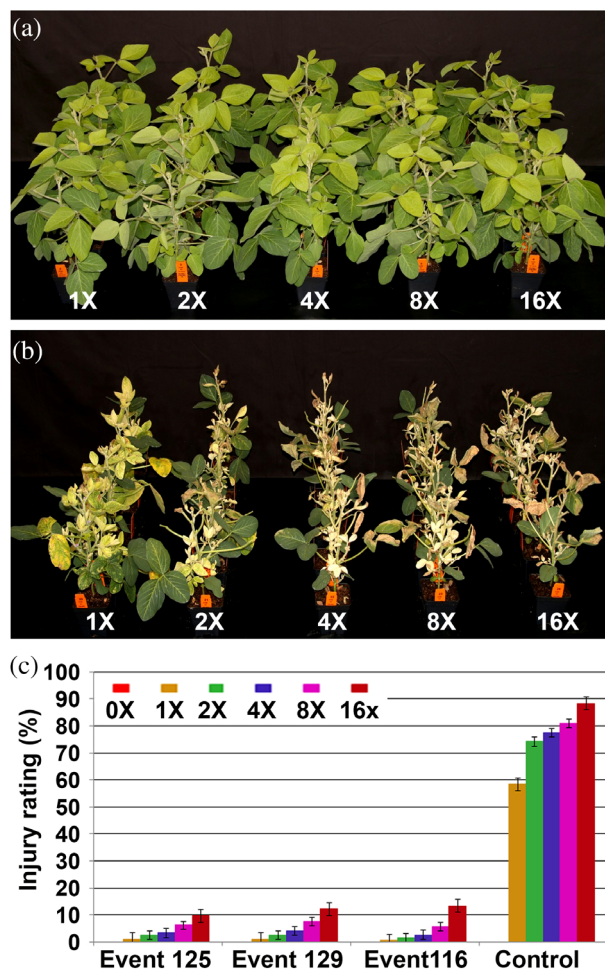
Figure 1. Constitutive overexpression of the triketone dioxygenase gene (*TDO*) in soybean confers commercial level tolerance to mesotrione. (A) Plants of transgenic event 125 of p35S::TDO treated with different rates of mesotrione, ranging from 1× to 16× the commercial rate. 1× commercial rate = 105 g ha^{-1} of mesotrione active ingredient. (B) Nontransgenic conventional soybean plants treated with the same rates of mesotrione as in (A). (C) Mesotrione-induced injury ratings in plants of p35S::TDO transgenic events and the conventional soybean control. Ratings were taken 13 days after mesotrione treatments at the V4 growth stage. Each bar shows the mean of eight replicates ±SE.

conducted using ^{14}C-mesotrione. As shown in Fig. 2(C), the percentage of radioactivity translocated from the treated first trifoliate to the apex (all tissues above the first trifoliate) kept increasing in conventional soybean plants and reached 28% of total radioactivity absorbed by the plants at 72 HAT. Radioactivity in the treated first trifoliates continued decreasing and reduced to 64% of total absorbed radioactivity at 72 HAT (Fig. 2(D)). A small percentage of absorbed radioactivity was also moved basipetally to unifoliates and roots in the conventional soybean plants (Fig. S2). In contrast, only a basal level of radioactivity was detected in the apexes, unifoliates, and roots of *TDO* transgenic plants at 72 HAT (Figs 2(C) and S2), and nearly all radioactivity was retained in the treated first trifoliates (Fig. 2(D)).

These two experiments (Figs 2 and S2) demonstrate that, similar to the movement in susceptible weeds,[18] mesotrione moves systemically in conventional soybean plants, especially towards emerging young leaf tissues, and causes herbicide injury. Overall,

these data show that overexpression of *TDO* in soybean prevents the systemic movement of mesotrione and overaccumulation of the herbicide in emerging young leaf tissues, which protects the plant from injury.

3.3 Ectopic expression of TDO protects HPPD from mesotrione-induced inhibition

Inhibition of HPPD by mesotrione results in the destruction of chlorophyll and classical bleaching symptoms.[14,18] A time-course study was conducted to evaluate the effect of TDO on HPPD protection in the apex. V1 growth stage plants with apexes covered by aluminum foil were sprayed with a 2× rate of mesotrione. Samples collected at specified time points after the treatment were analyzed using UPLC–MS/MS to detect and quantify mesotrione, hydroxy-mesotrione (mesotrione-OH), HPPA, HGA, AMBA, and MNBA. Similar to results from our radiolabeled study (Fig. 2(C)), the amount of mesotrione translocated to the apexes of *TDO* transgenic plants was at basal level at all time points (Fig. 3(A)). However, accumulation of mesotrione in the apexes of conventional soybean plants reached 10.2 nmol g^{-1} at 24 HAT and remained at 2.8 nmol g^{-1} at 72 HAT (Fig. 3(A)). Slow reduction of mesotrione in the apexes of conventional soybean plants at 72 HAT may be partially attributed to the slow catabolism of mesotrione in the apex and, potentially, some level of growth-related titration. Mesotrione-OH in the apexes of conventional soybean plants became detectable at low levels at 24 HAT (0.35 nmol g^{-1}) and increased to 1.55 nmol g^{-1} at 72 HAT (Fig. 3(B)). In contrast, there was no detectable mesotrione-OH in the apexes of *TDO* transgenic plants. This is most likely due to the quick turnover of mesotrione in the leaves exposed to the herbicide preventing it from translocating to apexes (Fig. 3(B)).

Due to slow catabolism, mesotrione mostly remains as an unaltered active form to inhibit HPPD when it translocates through the plant and accumulates in apical tissues of conventional soybean plants. The inhibition of HPPD in apexes can be evaluated by tracking the amount of HPPA and HGA. Starting from 3 HAT until 24 HAT, HPPA levels kept increasing in the apexes of conventional soybean plants and remained at elevated levels up to the last time point of this study, 72 HAT (Fig. 3(C)). Likewise, HGA levels quickly decreased to 0.65 nmol g^{-1} at 3 HAT in the apexes of conventional soybean plants and remained at this low level at all later time points (Fig. 3(D)). The observed changes of HPPA and HGA levels indicated that HPPD was inhibited by translocated mesotrione in the apexes of conventional soybean plants. In contrast, due to the lack of detectable translocation of mesotrione to apexes in *TDO* transgenic plants, the level of HPPA and HGA in the apexes was not perturbated, thus the function of HPPD in apexes of *TDO* transgenic plants was not affected (Fig. 3).

3.4 Ectopic expression of TDO converts mesotrione into metabolites similar to known classes of plant secondary metabolites

Converting mesotrione into AMBA via MNBA and other intermediates was reported as a path to metabolize mesotrione in corn plants, which are naturally resistant to the herbicide, and in soil, which is mediated by bacteria using enzymes such as nitro reductases.[24–26] However, only basal to low amounts of MNBA and AMBA were detected in the apexes of conventional soybean plants (Fig. S3). In addition, only low amounts of mesotrione-OH were detected in the apexes of conventional soybean plants which contained a much higher amount of translocated mesotrione at 24 and 72 HAT (Fig. 3(A),(B)). Slow deactivation of
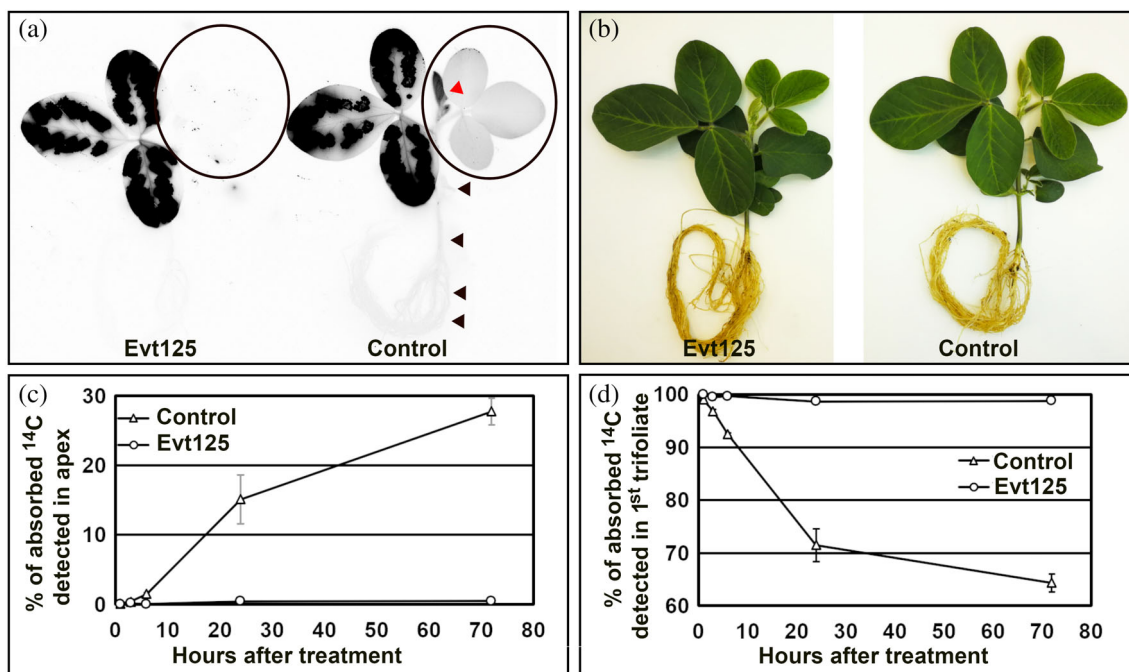
Figure 2. Overexpression of the triketone dioxygenase gene (*TDO*) in soybean plants prevents mesotrione translocation from treated trifoliate leaves to other tissues. (A) Radiograph of *TDO* transgenic (event 125) and conventional (control) plants at 30 h after treatment (HAT). ^{14}C-mesotrione was applied onto the first trifoliate leaves at the V1 growth stage. Shoot apex areas of *TDO* and control plants are circled. The red arrow points to the new emerging leaf of the control plant with high accumulation of translocated mesotrione and black arrows point to tissues with basipetal translocation of mesotrione in the control plant. (B) Image of the identical plants in (A) immediately before exposure to a phosphoscreen. (C) Percentage of the total absorbed radioactivity translocated to the shoot apex in a time-course study after the first trifoliate was treated with ^{14}C-mesotrione. Apexes were sampled at 1, 3, 6, 24, and 72 HAT. (D) Percentage of the total absorbed radioactivity retained in the first trifoliate at 1, 3, 6, 24, and 72 HAT. Open triangles, conventional soybean control plants; open circles, p35S::TDO transgenic event 125 (Evt125). Each datapoint represents the mean of four replicates ±SE.

mesotrione, either by converting it to AMBA via MNBA or mesotrione-OH, which has previously been shown to be mediated by cytochromes P450s and other enzymes in weeds,[27–30] makes conventional soybean very sensitive to mesotrione inhibition.

To better understand how mesotrione was metabolized in leaf tissues of conventional and *TDO* transgenic plants exposed to the herbicide, additional isotope tracing studies were conducted. First, a study using a mixture of ^{13}C- and ^{14}C-mesotrione to treat plants and identify mesotrione derivatives was conducted. Samples of treated first trifoliates of *TDO* transgenic event 125 and conventional soybean plants were analyzed using HPLC/RAD/MS–MS to detect expected compounds (e.g. mesotrione) as well as compounds with an elevated ^{13}C/^{12}C ratio (Fig. S4). A list of identifiable compounds including mesotrione and its derivatives was developed from this experiment (Table 1) and quantified in the following experiment.

To quantify the dynamic change of compounds listed in Table 1, a time-course study was conducted using ^{14}C-mesotrione-treated first trifoliate samples. Results from HPLC/RAD/MS–MS analysis demonstrated that mesotrione was rapidly catabolized in *TDO* transgenic plants (Fig. 4(B),(D),(F),(H)). This degradation process was confirmed in *TDO* transgenic plants developed from pCon::TDO, carrying *TDO* driven by a different constitutive promoter (Fig. S5(B),(D)). Metabolites with known or putative IDs in the samples were quantified. In treated trifoliates of *TDO* transgenic plants, mesotrione accounted for an average of 41% of the total absorbed radiation at 1 HAT, which quickly lowered and stabilized between 8.7% and 10.5% at 6 HAT and afterwards (Fig. 5(A)). In contrast, the percentage of absorbed radiation accounted for by mesotrione was 86% in treated trifoliates of conventional soybean plants at 1 HAT and slowly reduced with time but remained at 27% by 72 HAT (Figs 4(A),(C),(E),(G) and 5(A)).

Furthermore, the total percentage of radiation in extracts accounting for mesotrione and other identifiable metabolic derivatives was maintained at a similar level among samples of *TDO* transgenic plants collected from 1 to 72 HAT (70–77%). TDO-mediated biochemical processes are major paths to rapidly oxidize the majority of mesotrione applied and generally further convert oxidized mesotrione derivatives into tractable compounds in transgenic plants. In contrast, the total percentage of radiation in samples of conventional soybean plants attributed to mesotrione and other identifiable metabolic derivatives started at 89% of total radiation (86% mesotrione plus 3% of other metabolic derivatives) at 1 HAT and gradually reduced to 55% at 72 HAT. This suggests that, even though conventional soybean plants can metabolize mesotrione, it is an inefficient and complex process that leads to low-abundance unidentifiable derivatives (accounting for 45% of the total radiation at 72 HAT) and some identifiable metabolites such as 4-hydroxy-mesotrione (Fig. 5(A)).

Among the identifiable mesotrione derivatives in samples of conventional plants, MNBA and AMBA were observed at low abundances, 0.6–2.0% and 1.0–3.3%, respectively. This confirms that the conversion of mesotrione to AMBA via MNBA is a minor path to catabolize mesotrione in conventional soybean plants (Figs 5 and S5). Three additional identifiable mesotrione derivatives in conventional soybean samples were 4-hydroxy-mesotrione, 5-hydroxy-mesotrione, and xanthone; their levels reached 9.4%, 10.8%, and 6.7% of total radiation counts in extracts at 72 HAT, respectively (Figs 4 and 5(A)).
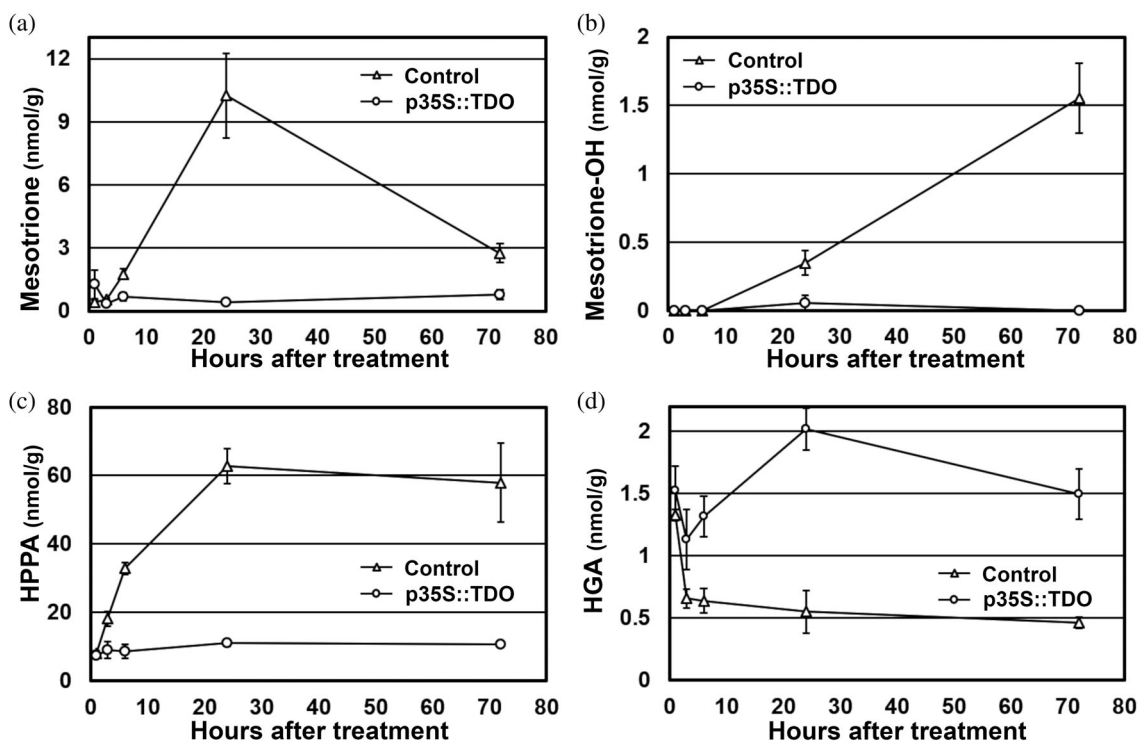
Figure 3. Overexpression of the triketone dioxygenase gene (*TDO*) in soybean protects hydroxyphenylpyruvate dioxygenase (HPPD) activity from mesotrione inhibition in the shoot apex. The shoot apexes of V1 growth stage plants were covered with aluminum foil and sprayed with a 2× commercial rate of mesotrione. Apexes were sampled at 1, 3, 6, 24, and 72 h after treatment. Mesotrione, mesotrione-OH, hydroxyphenylpyruvic acid (HPPA), and homogentisic acid (HGA) levels were measured in shoot apex samples not directly exposed to mesotrione treatment using HPLC. Quantification of (A) mesotrione, (B) mesotrione-OH, (C) HPPA – the substrate of HPPD, and (D) HGA, the product of HPPD in shoot apex. Open triangles, conventional soybean control; open circles, p35S::TDO transgenic events. Each datapoint represents the mean of three replicates ±SE.

Table 1. Mass and retention times of mesotrione derivatives with known and putative identifications in conventional soybean and *TDO* transgenic plants

#	Metabolites	Monoisotopic mass	Retention time (min)	Formula
0	Mesotrione	339.0413	36.35	C14H13NO7S
1	Mesotrione-OH (5OH)	355.0362	22.31	C14H13NO8S
2	Mesotrione-OH (4OH)	355.0362	24	C14H13NO8S
3	Xanthone-OH	306.0198	47.74	C14H10O6S
4	Acridone-OH	305.0358	37.99	C14H11NO5S
5	Xanthone-OH-glucosyl	468.0726	25.24	C20H20O11S
6	Acridone-OH-glucosyl	467.0886	24.7	C20H21NO10S
7	Xanthone-OH-glucosyl-malonyl	554.073	31.47	C23H22O14S
8	Acridone-glucosyl-malonyl	553.089	30.44	C23H23NO13S
9	Xanthone	290.0249	50.43	C14H10O5S
10	AMBA	215.0252	15.76	C8H9NO4S
11	MNBA	244.9994	9.97	C8H7NO6S

In addition to metabolic derivatives detected in conventional soybean plants, acridone-OH, xanthone-OH, and their glucosyl- and glucosyl-malonyl conjugates were detected in *TDO* transgenic samples collected at various time points. Acridone-OH, xanthone-OH, and conjugates of acridone and xanthone were likely formed after the TDO-mediated second oxidation of 5-hydroxy-mesotrione and, potentially, 4-hydroxy-mesotrione. These metabolites detected in *TDO* transgenic plants are similar to xanthone- and acridone-related plant secondary metabolites.[31,32] Conjugated xanthone and acridone continued to accumulate and reached 52% of the total radiation counts in samples of *TDO* transgenic plants at 72 HAT (Fig. 5(A)). A literature review, in combination with identifiable mesotrione derivatives in the datasets described above, allowed us to propose mesotrione metabolism pathways in conventional and *TDO* transgenic soybean plants (Figs 5(B) and S6).
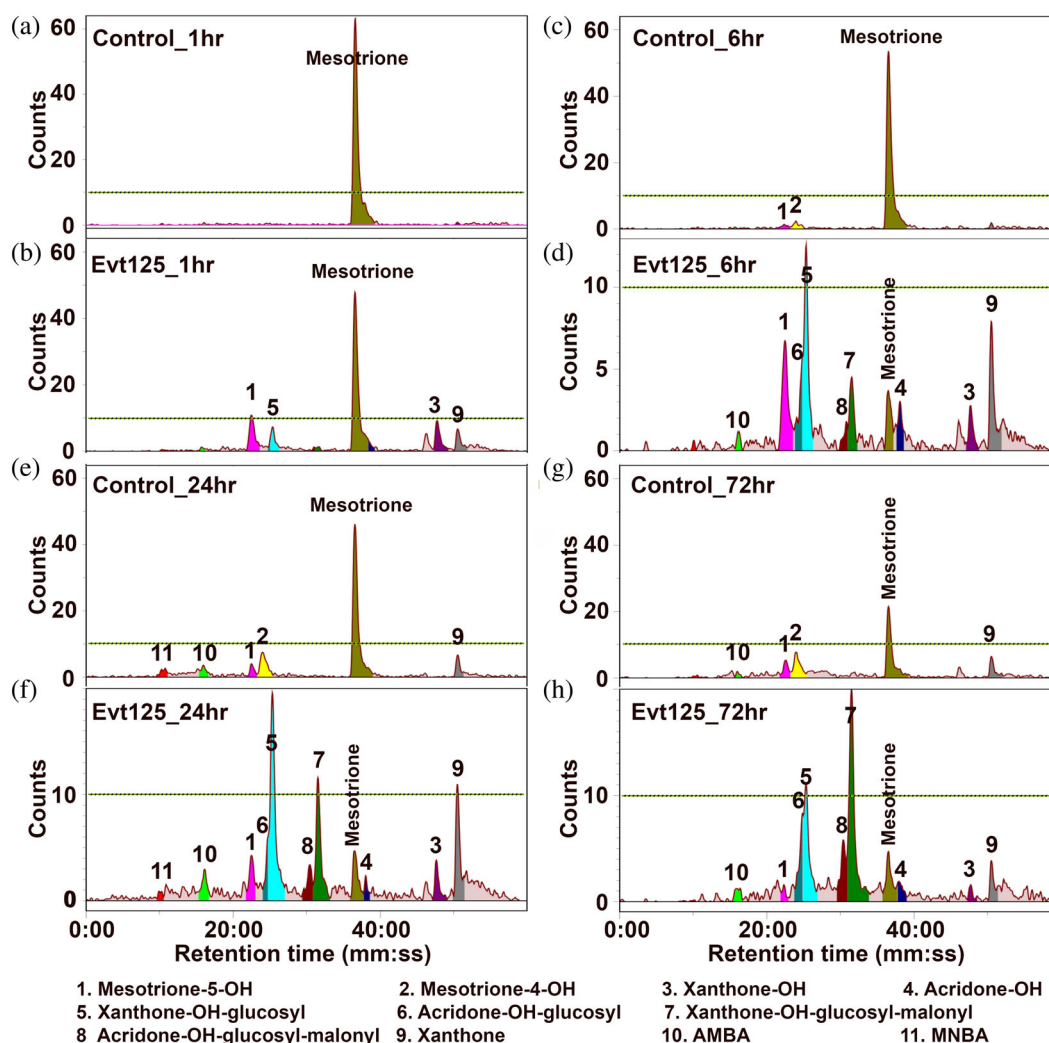
Figure 4. HPLC-RAD chromatograms of the first trifoliate leaves treated with ^{14}C-mesotrione. The first trifoliate was treated with ^{14}C-mesotrione at the V1 growth stage, washed, sampled at 1, 6, 24, and 72 h after treatment (HAT), and subjected to HPLC/RAD analysis. In all panels, the y axis is HPLC radiation count and the x axis is the retention time. (A), (C), (E), and (G) are representative chromatograms of conventional soybean control plant samples collected at 1, 6, 24, and 72 h after treatment, respectively. (B), (D), (F), and (H) are representative chromatograms of samples from p35S::TDO transgenic event 125 (Evt125) collected at 1, 6, 24, and 72 HAT. Metabolites with putative identities are numbered and highlighted in the same color in all panels. Putative identities of numbered peaks are listed at the bottom of chromatogram panels.

3.5 Ectopic expression of TDO prevents mesotrione-mediated inhibition of carotenoid biosynthesis

Mesotrione-induced inhibition of HPPD causes depletion of HGA, which subsequently leads to depletion of PQ and impairs the function of PDS and, thus, carotenoid biosynthesis.[17,18] Impaired carotenoid biosynthesis will ultimately lead to bleaching symptoms. However, leaves of conventional soybean plants fully expanded prior to mesotrione treatment stayed green for a much longer period of time, as shown in Figs 1 and 6(A), and in a previous report, while bleaching symptoms were visible in emerging leaves in just a couple of days after application.[33] To better understand the heterogenic responses among leaves at different developmental stages to the mesotrione treatment in conventional soybean plants and TDO-mediated protection, key metabolites of the carotenoid biosynthesis pathway (Fig. 6(A)) and chlorophyll a and b were quantified in samples of the first trifoliates (fully expanded prior to treatment) and apexes (emerging tissues at treatment) collected 3 days after a 2× mesotrione spray of V1 growth stage plants.

In the apexes of mesotrione-treated plants, all quantified metabolites showed significant differences ($P < 0.01$) between conventional and TDO transgenic plants (Fig. 6(B)–(J), column Apex). Accumulation of phytoene increased ~5.5-fold in conventional soybean plants compared to TDO transgenic plants due to the negative effect of PQ depletion on the function of PDS (Fig. 6(B), column Apex). β-Carotene was almost fully depleted (0.45 ppm) in the apexes of conventional plants while it was 256 ppm in TDO transgenic plants (Fig. 6(C), column Apex). Similarly, other xanthophylls were almost depleted and chlorophyll a and b were dramatically reduced in the apexes of conventional plants at 3 days after treatment (Fig. 6(D)–(J), column Apex).

In contrast to the apex, the phytoene level in the first trifoliate of conventional plants was not significantly different from that of TDO transgenic plants (Fig. 6(B)). Although β-carotene in treated first trifoliates of conventional plants was significantly lower than that of TDO plants (Fig. 6(C)), it was still ~2 times higher than that of untreated apex. One interesting observation was that zeaxanthin and antheraxanthin were significantly increased in the first
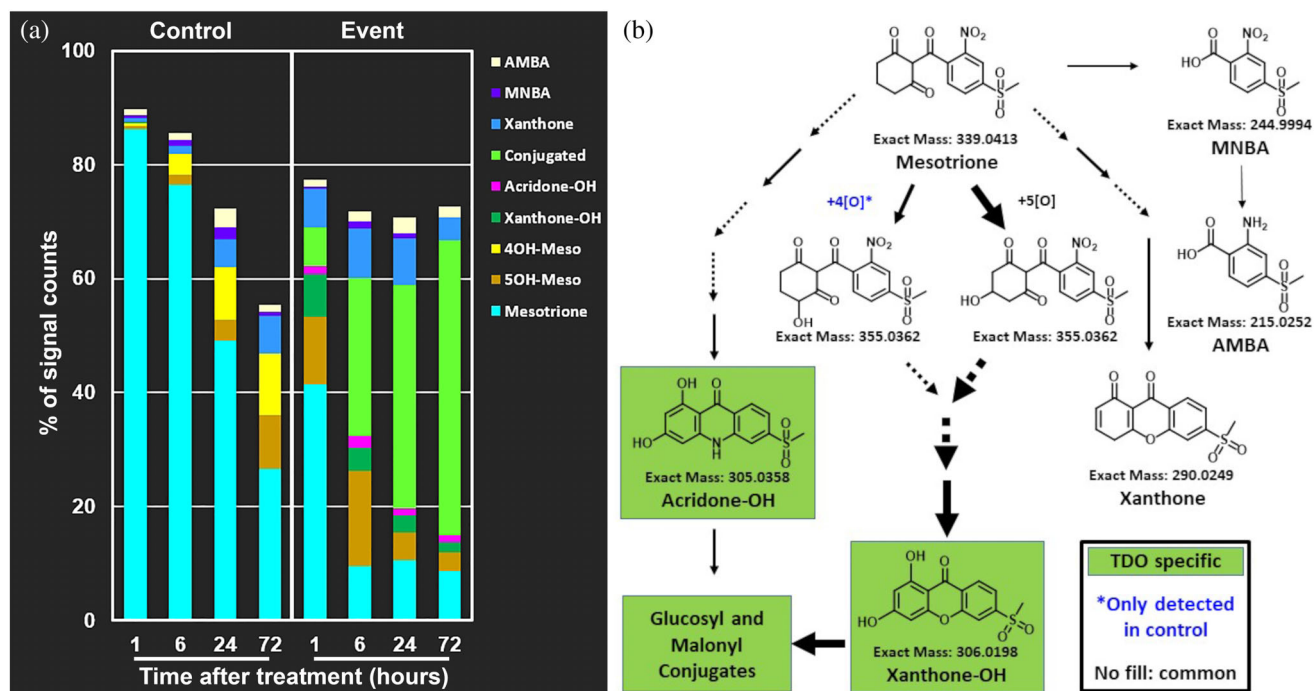
Figure 5. Relative abundance of mesotrione derivatives and the putative metabolic paths for detoxifying mesotrione in ^{14}C-mesotrione-treated first trifoliates of *TDO* transgenic plants and conventional soybean control plants. Metabolites with putative identifications were analyzed and quantified using HPLC-RAD. (A) Relative abundance of metabolites with putative identities in ^{14}C-mesotrione-treated first trifoliates. Stacked bars show the percentage abundance of metabolites with putative identities in control plants (left panel) and *TDO* transgenic event 125 (right panel) at 1, 6, 24, and 72 h after ^{14}C-mesotrione treatment. Each data point is the mean of four replicates. (B) Putative metabolic paths for turning over mesotrione in *TDO* and control plants. The thickness of the arrows indicates the relative strength of the path. Solid arrows point to detected metabolites with the expected molecular mass while dashed-line arrows point to hypothetical intermediates. Metabolites highlighted in green were only detected in the p35S::TDO transgenic event. *Note: mesotrione-4OH was only detected in control plants.

4 DISCUSSION

While the development and deployment of HT crops, especially GT crops, has revolutionized modern agriculture, broad adoption of HT crops with a single HT mode of action has contributed to the rapid rise of herbicide-resistant weeds.[6,10] In response to the growing pressure of herbicide-resistant weeds, crops carrying two to three HT traits have been developed.[3] Developing crops with additional modes of action of HT traits will provide farmers with more options to manage herbicide-resistant weeds and help slow the pace of weed species evolving resistance. HPPD-inhibiting herbicides including mesotrione have favorable environmental and toxicological profiles,[21] making them excellent candidates for transgenic tolerance trait development.

The TDO-mediated mesotrione tolerance trait presented here is different from those traits previously developed using herbicide insensitive HPPDs.[33–36] TDO directly deactivates mesotrione molecules by converting them into noninhibitory metabolites that are further converted into metabolites similar to known classes of plant secondary metabolites in soybean plants (Figs 5 and S6). Similar to insensitive HPPD, which confers tolerance to multiple

HPPD-inhibiting herbicides in transgenic plants,[33] expression of *HIS1* in transgenic rice plants showed tolerance to multiple triketone herbicides.[22] In this study, overexpression of *TDO* in soybean also confers tolerance, in addition to mesotrione, to two other triketone HPPD inhibitors, tembotrione and sulcotrione (Fig. S7).

Conventional soybean is highly susceptible to mesotrione even though it is capable of catabolizing mesotrione into a few detectable derivatives at a slow rate. Among these mesotrione derivatives, AMBA and MNBA are minor constituents compared to 4-hydroxy-mesotrione and 5-hydroxy-mesotrione, which are potentially formed through oxidation by unidentified soybean cytochrome p450 monooxygenases and perhaps other unknown enzymes, as has been previously reported in weeds.[27–30] At low levels overall, accumulation of 4-hydroxy-mesotrione and 5-hydroxy-mesotrione in conventional soybean increased with time (Figs 3(B) and 5(A)). This suggests that conventional soybean lacks a suitable dioxygenase to further oxidize these two mesotrione derivatives.

Conversely, TDO in transgenic plants first oxidizes mesotrione on the 5-carbon to convert mesotrione into 5-hydroxy-mesotrione, subsequently introduces a second oxidation, and leads to the generation of oxy-mesotrione (Figs 5(B) and S6).[23] However, unlike data from conventional soybean plants, 4-hydroxy-mesotrione was not detected in samples of *TDO* transgenic plants (Fig. 5(A)). One possible explanation is that TDO can rapidly introduce a second oxidation at the 5-carbon position of 4-hydroxy-mesotrione, causing this intermediate to be undetectable. After the second oxidation of mesotrione, oxy-mesotrione is generated
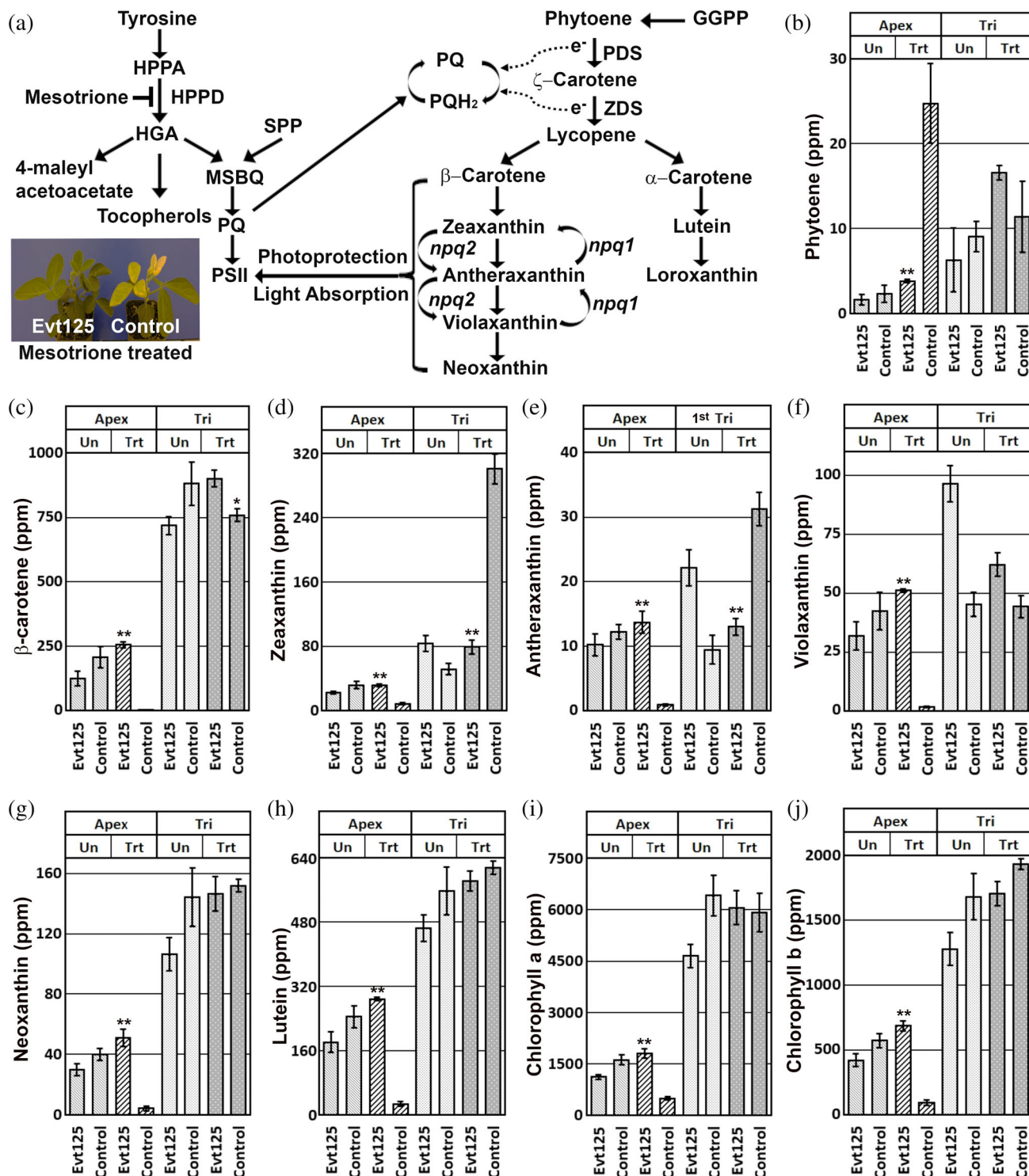
Figure 6. Overexpression of the triketone dioxygenase gene (*TDO*) protects carotenoid biosynthesis in the shoot apex from being negatively affected by mesotrione-mediated inhibition of HPPD. (A) Interconnection between tyrosine degradation and carotenoid biosynthesis pathways, adapted from Niyogi *et al.* and Stacey *et al.*[16,42] Mesotrione inhibits HPPD and affects the function of PDS through depletion of PQ. The image in (A) was taken 5 days after mesotrione treatment at the V1 growth stage. (B)–(J) Quantification of metabolites in the carotenoid biosynthesis pathway and chlorophyll a and b. All samples were collected at 72 h after a 2× commercial rate of mesotrione treatment at V1 growth stage. In each panel, sample 'Apex' includes all tissues above the node of the first trifoliate and sample 'First Tri' includes all tissues of the first trifoliate. Comparisons between control and p35S::TDO transgenic event 125 (Evt125) were defined within the ANOVA and tested using *t*-tests. Each bar represents the mean of three replicates ±SE. Significant difference between TDO event and the corresponding control at **$P \leq 0.01$ and *$P \leq 0.05$.

after losing a water molecule and forms xanthone-OH in the *TDO* transgenic plants (Figs 5(A),(B) and S6). Similarly, TDO is hypothesized to convert the mesotrione-derived MW291.06 intermediate into acridone-OH after the second oxidation (Figs 5(A),(B) and S6). Xanthone-OH and acridone-OH are conjugated with glucosyl and malonyl groups (Figs 5(A),(B) and S6). Most likely due to the poor

aqueous solubility of these metabolites,[32,37–39] xanthone and acridone derivatives are immobilized in tissues where these metabolites are formed (Fig. 2). There is also a minor hypothetical path to convert mesotrione into xanthone via a MW292.04 intermediate (Figs 5(B) and S6). Overall, the rapid conversion of mesotrione into noninhibitory metabolites through double oxidations in tissues exposed to the herbicide is the key feature of the TDO-mediated mesotrione tolerance in soybean.

Rapid degradation of mesotrione in *TDO* transgenic plants minimized the effect of the herbicide on carotenoid biosynthesis and chlorophyll accumulation in vulnerable newly emerging tissues in the apex (Fig. 6). Conversely, mesotrione caused classical bleaching phenotypes in young emerging tissues of conventional soybean plants due to the depletion of PQ caused by depletion of HGA (Figs 1(B), 3(D), and 6(A)). Similar to the effect of isoxaflutole-mediated inhibition of HPPD,[40] mesotrione treatment impairs the function of PDS. The level of phytoene, the substrate of PDS, significantly increased in the herbicide-treated apexes of conventional soybean plants while the level of carotenoids and chlorophylls was greatly reduced (Fig. 6).

In contrast to the emerging leaf tissues, fully expanded leaves of conventional soybean plants are less responsive to mesotrione treatment and slowly develop herbicide-induced bleaching symptoms (Fig. 1). This can be, partially, attributed to the temporospatial expression profile of soybean PDS genes. There are two PDS genes in soybean: Glyma.11G253000, which is highly expressed in young emerging leaves, flowers and developing pods but not in matured leaves, and Glyma.18G003900, which is mostly expressed in flowers[41] (Soybase.org). An unexpected observation is that accumulation of zeaxanthin and antheraxanthin significantly increased in the treated first trifoliates of conventional soybean plants (Fig. 6(D),(E)). This is most likely the result of xanthophyll cycle-mediated rebalancing, which involves the *npq1*-like genes among others.[42] Mature leaves of conventional soybean plants are slow to respond to mesotrione treatment due to the minimal expression of PDS genes in those leaves in combination with the slow formation of noninhibitory 4-hydroxy-mesotrione and 5-hydroxy-mesotrione,[23,27,28] a relatively high level reserve of xanthophylls, and the rebalance of xanthophylls.

5 CONCLUSION

Overall, mesotrione has a favorable environmental and toxicological profile,[21] is familiar to farmers as a selective herbicide in corn production for both pre- and post-emergence weed control,[18] and has limited known resistance among weed species[43] (Weedscience.org). TDO rapidly deactivates mesotrione in leaf tissues exposed to the herbicide and confers tolerance to up to 16× the commercial application rate (Fig. 1). The chemical and agronomic characteristics of mesotrione in combination with *TDO*-mediated mesotrione tolerance via deactivation makes the mesotrione tolerance trait described here a new option for farmers to effectively manage difficult-to-control weeds in soybean acres. Moreover, this *TDO*-mediated mesotrione tolerance trait can potentially be adapted to other important dicot crops (e.g. cotton) for effective weed management.

DATA AVAILABILITY STATEMENT

The data that supports the findings of this study are available in the supplementary material of this article

SUPPORTING INFORMATION

Supporting information may be found in the online version of this article.

REFERENCES

1 Popp J, Pető K and Nagy J, Pesticide productivity and food security. A review. *Agron Sustain Dev* **33**:243–255 (2013).
2 Green JM, The benefits of herbicide-resistant crops. *Pest Manag Sci* **68**: 1323–1331 (2012).
3 Nandula VK, Herbicide resistance traits in maize and soybean: current status and future outlook. *Plants* **8**:337 (2019).
4 Van Deynze B, Swinton SM and Hennessy DA, Are glyphosate-resistant weeds a threat to conservation agriculture? Evidence from tillage practices in soybeans. *Am J Agric Econ* **104**:645–672 (2022).
5 Yu Z, Lu C, Hennessy DA, Feng H and Tian H, Impacts of tillage practices on soil carbon stocks in the US corn-soybean cropping system during 1998 to 2016. *Environ Res Lett* **15**:014008 (2020).
6 Dill GM, CaJacob CA and Padgette SR, Glyphosate-resistant crops: adoption, use and future considerations. *Pest Manag Sci* **64**:326–331 (2008).
7 Green JM and Owen MDK, Herbicide-resistant crops: utilities and limitations for Herbicide-resistant Weed Management. *J Agric Food Chem* **59**:5819–5829 (2011).
8 Carpenter JE, Peer-reviewed surveys indicate positive impact of commercialized GM crops. *Nat Biotechnol* **28**:319–321 (2010).
9 Peterson MA, Collavo A, Ovejero R, Shivrain V and Walsh MJ, The challenge of herbicide resistance around the world: a current summary. *Pest Manag Sci* **74**:2246–2259 (2018).
10 Beckie HJ, Herbicide resistance in plants. *Plants* **9**:435 (2020).
11 Pannell DJ, Tillie P, Rodríguez-Cerezo E, Ervin D and Frisvold GB, Herbicide resistance: economic and environmental challenges. *AgBioForum* **19**:136–155 (2016).
12 Larue CT, Ream JE, Zhou X, Moshiri F, Howe A, Goley M, *et al.*, Microbial HemG-type protoporphyrinogen IX oxidase enzymes for biotechnology applications in plant herbicide tolerance traits. *Pest Manag Sci* **76**: 1031–1038 (2020).
13 Beckie HJ, Ashworth MB and Flower KC, Herbicide resistance management: recent developments and trends. *Plants* **8**:161 (2019).
14 van Almsick A, New HPPD-inhibitors – a proven mode of action as a new hope to solve current weed problems. *Outlooks Pest Manag* **20**:27–30 (2009).
15 Norris SR, Shen X and Della Penna D, Complementation of the Arabidopsis pds1 mutation with the gene encoding p-hydroxyphenylpyruvate dioxygenase. *Plant Physiol* **117**:1317–1323 (1998).
16 Stacey MG, Cahoon RE, Nguyen HT, Cui Y, Sato S, Nguyen CT, *et al.*, Identification of homogentisate dioxygenase as a target for vitamin E biofortification in oilseeds. *Plant Physiol* **172**: 1506 (2016), 1518.
17 Norris SR, Barrette TR and DellaPenna D, Genetic dissection of carotenoid synthesis in arabidopsis defines plastoquinone as an essential component of phytoene desaturation. *Plant Cell* **7**:2139–2149 (1995).
18 Mitchell G, Bartlett DW, Fraser TEM, Hawkes TR, Holt DC, Townson JK *et al.*, Mesotrione: a new selective herbicide for use in maize. *Pest Manag Sci* **57**:120–128 (2001).
19 Carles L, Joly M, Joly P and Herbicide M, Efficiency, effects, and fate in the environment after 15 years of agricultural use. *CLEAN – Soil Air Water* **45**:1700011 (2017).
20 Dyson JS, Beulke S, Brown CD and Lane MCG, Adsorption and degradation of the weak acid mesotrione in soil and environmental fate implications. *J Environ Qual* **31**:613–618 (2002).
21 Meazza G, Scheffler BE, Tellez MR, Rimando AM, Romagni JG, Duke SO, *et al.*, The inhibitory activity of natural products on plant

p-hydroxyphenylpyruvate dioxygenase. *Phytochemistry* **60**: 281–288 (2002).

22 Maeda H, Murata K, Sakuma N, Takei S, Yamazaki A, Karim MR, *et al.*, A rice gene that confers broad-spectrum resistance to *β*-triketone herbicides. *Science* **365**: 393–396 (2019).

23 Duff S, Zheng M, Taylor C, Chen D, Mamanella P, Duda D et al., Structural and functional characterization of tri-ketone dioxygenase from Oryza sativa, in preparation. Forthcoming.

24 Durand S, Sancelme M, Besse-Hoggan P and Combourieu B, Biodegradation pathway of mesotrione: complementarities of NMR, LC–NMR and LC–MS for qualitative and quantitative metabolic profiling. *Chemosphere* **81**:372–380 (2010).

25 Carles L, Besse-Hoggan P, Joly M, Vigouroux A, Moréra S and Batisson I, Functional and structural characterization of two *Bacillus megaterium* nitroreductases biotransforming the herbicide mesotrione. *Biochem J* **473**:1443–1453 (2016).

26 Alferness P and Wiebe L, Determination of mesotrione residues and metabolites in crops, soil, and water by liquid chromatography with fluorescence detection. *J Agric Food Chem* **50**:3926–3934 (2002).

27 Kaundun SS, Hutchings S-J, Dale RP, Howell A, Morris JA, Kramer VC, *et al.*, Mechanism of resistance to mesotrione in an *Amaranthus tuberculatus* population from Nebraska, USA. *PLOS ONE* **12**: e0180095 (2017).

28 Ma R, Kaundun SS, Tranel PJ, Riggins CW, McGinness DL, Hager AG *et al.*, Distinct detoxification mechanisms confer resistance to mesotrione and atrazine in a population of waterhemp. *Plant Physiol* **163**: 363–377 (2013).

29 Nakka S, Godar AS, Wani PS, Thompson CR, Peterson DE, Roelofs J *et al.*, Physiological and molecular characterization of hydroxyphenylpyruvate dioxygenase (HPPD)-inhibitor resistance in *Palmer amaranth* (*Amaranthus palmeri* S.Wats.). *Front Plant Sci* **8**:555 (2017).

30 Küpper A, Peter F, Zöllner P, Lorentz L, Tranel PJ, Beffa R *et al.*, Tembotrione detoxification in 4-hydroxyphenylpyruvate dioxygenase (HPPD) inhibitor-resistant palmer amaranth (*Amaranthus palmeri* S. wats.). *Pest Manag Sci* **74**:2325–2334 (2018).

31 Alhassan A, Abdullahi M, Uba A and Umar A, Prenylation of aromatic secondary metabolites: a new frontier for development of novel drugs. *Trop J Pharm Res* **13**:8 (2014).

32 Vieira LMM and Kijjoa A, Naturally-occurring xanthones: recent developments. *Curr Med Chem* **12**:2413–2446 (2005).

33 Siehl DL, Tao Y, Albert H, Dong Y, Heckert M, Madrigal A, *et al.*, Broad 4-hydroxyphenylpyruvate dioxygenase inhibitor herbicide tolerance in soybean with an optimized enzyme and expression cassette. *Plant Physiol* **166**: 1162 (2014), 1176.

34 Dreesen R, Capt A, Oberdoerfer R, Coats I and Pallett KE, Characterization and safety evaluation of HPPD W336, a modified 4-hydroxyphenylpyruvate dioxygenase protein, and the impact of its expression on plant metabolism in herbicide-tolerant MST-FGØ72-2 soybean. *Regul Toxicol Pharmacol* **97**:170–185 (2018).

35 Hawkes TR, Langford MP, Viner R, Blain RE, Callaghan FM, Mackay EA, *et al.*, Characterization of 4-hydroxyphenylpyruvate dioxygenases, inhibition by herbicides and engineering for herbicide tolerance in crops. *Pestic Biochem Physiol* **156**: 9–28 (2019).

36 Kramer CM, Launis KL, Traber MG and Ward DP, Vitamin E levels in soybean (*Glycine max* (L.) Merr.) expressing a p-hydroxyphenylpyruvate gene from oat (*Avena sativa* L.). *J Agric Food Chem* **62**:3453–3457 (2014).

37 Taguchi G, Ubukata T, Nozue H, Kobayashi Y, Takahi M, Yamamoto H *et al.*, Malonylation is a key reaction in the metabolism of xenobiotic phenolic glucosides in Arabidopsis and tobacco. *Plant J* **63**:1031–1041 (2010).

38 Ramesh Kumar MK, Chemistry of acridone and its analogues: a review. *J Chem Pharm Res* **3**:14 (2011).

39 Ho LY, Lim YY, Tan CP and Siow LF, Comparison of physicochemical properties and aqueous solubility of xanthone prepared via oil-in-water emulsion and complex coacervation techniques. *Int J Food Prop* **21**:784–798 (2018).

40 Pallett KE, Little JP, Sheekey M and Veerasekaran P, The mode of action of isoxaflutole: I. physiological effects, metabolism, and selectivity. *Pestic Biochem Physiol* **62**:113–124 (1998).

41 Du H, Zeng X, Zhao M, Cui X, Wang Q, Yang H et al., Efficient targeted mutagenesis in soybean by TALENs and CRISPR/Cas9. *J Biotechnol* **217**:90–97 (2016).

42 Niyogi KK, Grossman AR and Björkman O, Arabidopsis mutants define a central role for the xanthophyll cycle in the regulation of photosynthetic energy conversion. *Plant Cell* **10**:1121–1134 (1998).

43 Ndikuryayo F, Moosavi B, Yang W-C and Yang G-F, 4-Hydroxyphenylpyruvate dioxygenase inhibitors: from chemical biology to agrochemicals. *J Agric Food Chem* **65**:8523–8537 (2017).